## Accelerators, Beamlines, Experimental Apparatus, and Experimental Techniques

# Experimental Apparatus

# Correction of Non-Linearity in Detectors for Electron Spectroscopy

N. Mannella[1,2], S. Marchesini[2], S.-H. Yang[2], B.S. Mun[1,2], A.W. Kay[1,2,#], T. Gresch[2,3], A. Rosenhahn[2] and C.S. Fadley[1,2]

[1]Dept. of Physics, University of California-Davis, Davis, CA 95616
[2]Materials Sciences Division, Lawrence Berkeley National Laboratory, Berkeley, CA 94720
[3]Institute of Physics, University of Zurich, Zurich, Switzerland
[#]Present address: Intel Corporation, Portland, OR

## INTRODUCTION

The intensity levels reached in many third-generation synchrotron radiation experiments on solids have been found to exceed the linear response range of the final detection system involved. In electron spectroscopy, Seah and co-workers have previously discussed methods for detecting such non-linearity, including measurements with laboratory x-ray sources [1]. As a particular case involving synchrotron radiation, non-linearity has been noticed by several groups in using the Gammadata/Scienta electron spectrometers, with this behavior extending even to fairly low countrates [2-8]. For example, prior work on multi-atom resonant photoemission (MARPE) by several groups was strongly affected by this particular non-linearity [3-6]. While data related to the MARPE effect have been corrected for such non-linearities in prior publications [6b,7,8], we have found that other measurements such as the quantitative analysis of complex oxides via core-level intensities can be strongly influenced by this non-linearity, even when the exciting energy is far away from any resonance [9]. Similarly, measurements of relative intensities in angle-resolved valence spectra can also be significantly altered [10]. It is thus of interest to develop accurate and broadly utilizable procedures for correcting for non-linearity with any detection system. Although we will use one spectrometer system as an example, the methodologies discussed here should be useful for many other cases.

## CORRECTION METHODOLOGIES AND EXPERIMENTAL RESULTS

In Figure 1(a), we show broad-range survey spectra from a Cu(110) sample, as excited by Al K$\alpha$ radiation with various power levels and detected by a Scienta SES200 spectrometer and its standard microchannel-plate/phosphor/CCD detection system. Since the high voltage was held constant, this is verified experimentally to lead to x-ray flux being proportional to power [7]. The various spectra have been normalized to one another at the lowest-countrates, just above the valence region. If the detector were linear, all spectra should lie on top of one another, but it is evident that they are not, with factors of up to 4x separating them in the higher intensity regions at lower kinetic energy.

We now consider two methods for correcting for non-linearity in such spectra:

1. Measurement of flat-background reference intensity as a function of incident x-ray flux: In the most obvious method, a flat background region in a spectrum from a sample with a stable surface can simply be measured as a function of incident x-ray flux, with non-linearity then being reflected in any deviation of a plot of measured intensity vs. x-ray flux from a straight line [7]. One might term this a "partial yield" measurement of detector response. This curve can then be fit to a convenient polynomial function such that any non-linearity can be described finally via:

$$I_m(I_t, I_x) = b_0 + b_1 I_t(I_x) + \sum_{n=2}^{n_{max}} b_n I_t(I_x), \tag{1}$$

where $I_m$ = the measured countrate, $I_t$ = the true countrate, $I_x$ = the incident x-ray flux, the $b_n$ are empirical expansion coefficients, and $n_{max}$ is some maximum order chosen to adequately fit the data (roughly 5 in one prior analysis [7]). The coefficient $b_0$ thus represents the dark current in the absence of any excitation, and this will often be negligible, or at least can be simply subtracted from all measurements. The overall counting efficiency $\varepsilon$ is now defined simply as

$$\varepsilon(I_m) = \frac{I_m(I_t, I_x) - b_0}{I_t(I_x)} = b_1 + \sum_{n=2}^{n_{max}} b_n I_t^{n-1}(I_x). \tag{2}$$

Actual measured spectra can now be generally written as vectors $[I_{mi}(E_i)]$ over different energies $E_i$, and can be corrected to yield true spectra $[I_{ti}(E_i)]$ simply by dividing by $\varepsilon$, or

$$I_{ti}(E_i) = [\varepsilon(I_{mi})]^{-1} I_{mi}(E_i) \equiv \delta(I_{mi}) I_{mi}(E_i), \tag{3}$$

where the quantity $\delta(I_{mi})$ is defined by this equation.

Some measured vs. true countrates derived in this way are shown in Figure 1(c), and at minimum a significant quadratic correction term is evident. This procedure has been used in a prior analysis of detector non-linearity by Kay and co-workers [7,8], and it is found to yield excellent correction for such effects in the Scienta system, including the MARPE data discussed previously.

2. Analysis of broad-scan survey spectra at different incident x-ray fluxes:

Consider a set of $N$ survey spectra $I_{mi}^j(I_x^j, E_j)$ measured on the same sample, with incident fluxes $j = 1, 2, \ldots, N$, as illustrated shown in Figure 1(a). The intensities here span a range of approximately 40x, thus sampling the detector response very fully. We further assume that the true countrate $I_{ti}^j$ (minus dark current as needed) for a given flux $I_x^j$, and energy $E_i$, can be expressed via a simple proportionality to flux, and that the true spectra can also be described by another power series in the measured spectra, as

$$I_{ti}^j(I_x^j, E_i) = I_x^j I_0(E_i) = \sum_{k=1}^{P} a_i I_{mi}^k(E_i), \tag{4}$$

where $I_0(E_i)$ = the true spectral shape in energy, $j = 1, 2, \ldots, N$; $i = 1, 2, \ldots, M$ = no. of channels in energy, and $P$ is the maximum order of the polynomial needed to adequately describe the data (roughly 9 as a conservative number). Further assuming that the detector is linear at very low count rates such that, and then substituting for $I_{ti}^1$ and rearranging, permits expressing the data for all N spectra as:

$$\underbrace{-\left[\frac{I_{mi}(I_x^1, E_i)}{I_x^1} - \frac{I_{mi}(I_x^j, E_i)}{I_x^j}\right]}_{=\mathbf{B}} = \sum_{k=2}^{P} \underbrace{\left[\frac{I_{mi}^k(I_x^1, E_i)}{I_x^1} - \frac{I_{mi}^k(I_x^j, E_i)}{I_x^j}\right]}_{=\mathbf{M}} \underbrace{a_i}_{=\mathbf{A}}. \tag{5}$$

In matrix form, $\mathbf{B}$ is an $(N-1)\bullet M$ long column vector, $\mathbf{M}$ an $(N-1)\bullet M$ by $(P-1)$ matrix, and $\mathbf{A}$ a $(P-1)$ long column vector. Eq. (5) is an over-determined system of linear equations and can be solved for the maximum likelihood $a_i$'s in $\mathbf{A}$ by finding the minimum of $|\mathbf{B} - \mathbf{MA}|^2$, *i.e.* by solving for $0 = \nabla_A|\mathbf{B}-\mathbf{MA}|^2 = 2\mathbf{M}^\mathbf{T}\mathbf{M} - 2\mathbf{M}^\mathbf{T}\mathbf{B}$ (superscript $\mathbf{T}$ = transpose). The polynomial coefficients in can by obtained by a standard "LU" decomposition [11] or simply by matrix inversion:

$$\mathbf{A} = (\mathbf{M}^\mathbf{T}\mathbf{M})^{-1}\mathbf{M}^\mathbf{T}\mathbf{B}. \tag{6}$$

where $\left(\mathbf{M}^{\mathrm{T}}\mathbf{M}\right)$ is a small $\left(P-1\right)$ by $\left(P-1\right)$ matrix. For better numerical precision in the matrix inversion, the measured counts should vary from 0 to 1, which can be achieved by trivial normalization.

Some results obtained with both methods are shown in Figure 1(d), where the true counts are plotted as a function of measured counts, and essentially identical results for the curve are found from both methods. Finally, in Figure 1(b), we show the same spectra as Figure 1(a), but with the correction applied: it is clear that all normalized spectra for different fluxes coincide to a high accuracy, thus permitting quantitative spectroscopy to be performed with this detector.

## CONCLUSIONS

In summary, we have presented two distinct methods for correcting for non-linearity in detection systems, and demonstrated their validity for the specific case of the Scienta SES 200 spectrometer. Applications to this and other spectrometer systems for electrons and soft x-rays should be possible.

## REFERENCES


1. (a) M.P. Seah, M. Tosa, Surf. Interface. Anal. **18** (1992) 240; (b) M.P. Seah, I.S. Gilmore, S.J. Spencer, J. Electron Spectrosc. **104** (1999) 73-89.
2. M.P. Seah, M.Tosa, Surf. Interface. Anal. 18 (1992) 240; (b) M.P. Seah, I.S. Gilmore, S.J. Spencer, J. Electron Spectrosc. 104 (1999) 73-89.
3. A. Kay, E. Arenholz, B.S. Mun, F.J. Garcia de Abajo, C.S. Fadley, R. Denecke, Z. Hussain, and M.A. Van Hove, *Science* **281**, 679(1998).
4. E. Arenholz, A.W. Kay, C.S. Fadley, M.M. Grush, T.A. Callcott, D.L. Ederer, C. Heske, and Z. Hussain, *Phys. Rev. B* **61**, 7183 (2000).
5. A. Kikas, E. Nommiste, R. Ruus, A. Saar, and I. Martinson, Sol. St. Commun. **115**, 275 (2000).
6. (a) M.G. Garnier, N. Witkowski, R. Denecke, D. Nordlund, A. Nilsson, M. Nagasono, and N. Mårtensson, and A. Föhlisch, Maxlab Annual Report for 1999 and private communication correcting this data; (b) D. Nordlund, M.G. Garnier, N. Witkowski, R. Denecke, A. Nilsson, M. Nagasono, N. Martensson, A. Fohlisch, Phys. Rev. B 63, 121402 (2001).
7. A.W. Kay, Ph.D. dissertation (University of California-Davis, September, 2000), Chapters 4 and 5.
8. A.W. Kay, F.J. Garcia de Abajo, S.H. Yang, E. Arenholz, B.S. Mun, M.A. Van Hove, Z. Hussain, and C.S. Fadley, Physical Review B **63**, 5119 (2001), and Proceedings of the Eighth International Conference on Electronic Spectroscopy and Structure, J. Electron Spectrosc. **114**, 1179 (2001).
9. N. Mannella et al., private communication.
10. D. Dessau and Y. Chuang, private communication.
11. W. H. Press, S. A. Teukolsky, W. T. Vetterling, B. P. Flannery, "Numerical Recipes in C: The Art of Scientific Computing", Cambridge University Press, New York, 1992, pp. 43-50.



This work was supported by the U.S. Department of Energy, Office of Science, Office of Basic Energy Sciences, Materials Sciences Division, under Contract No. DE-AC03-76SF00098..



Principal investigator: Norman Mannella, Department of Physics UC Davis, and Materials Sciences Division, Lawrence Berkeley National Laboratory. Email: norman@electron.lbl.gov. Telephone: 510-486-5446

Figure 1. (a) Survey spectra from a Cu(110) sample, obtained with AlKα excitation at various x-ray powers and constant voltage, normalized to be equal at the lowest countrates near zero binding energy. (b) Survey spectra for the four lowest power settings after non-linearity correction. (c) Plot of true countrate vs. measured countrate, as derived from Method 1. Countrates expressed in Hz per pixel in the CCD camera [7,8]. (d) Plot of measured countrate vs. true countrate as derived from both Methods 1 and 2.

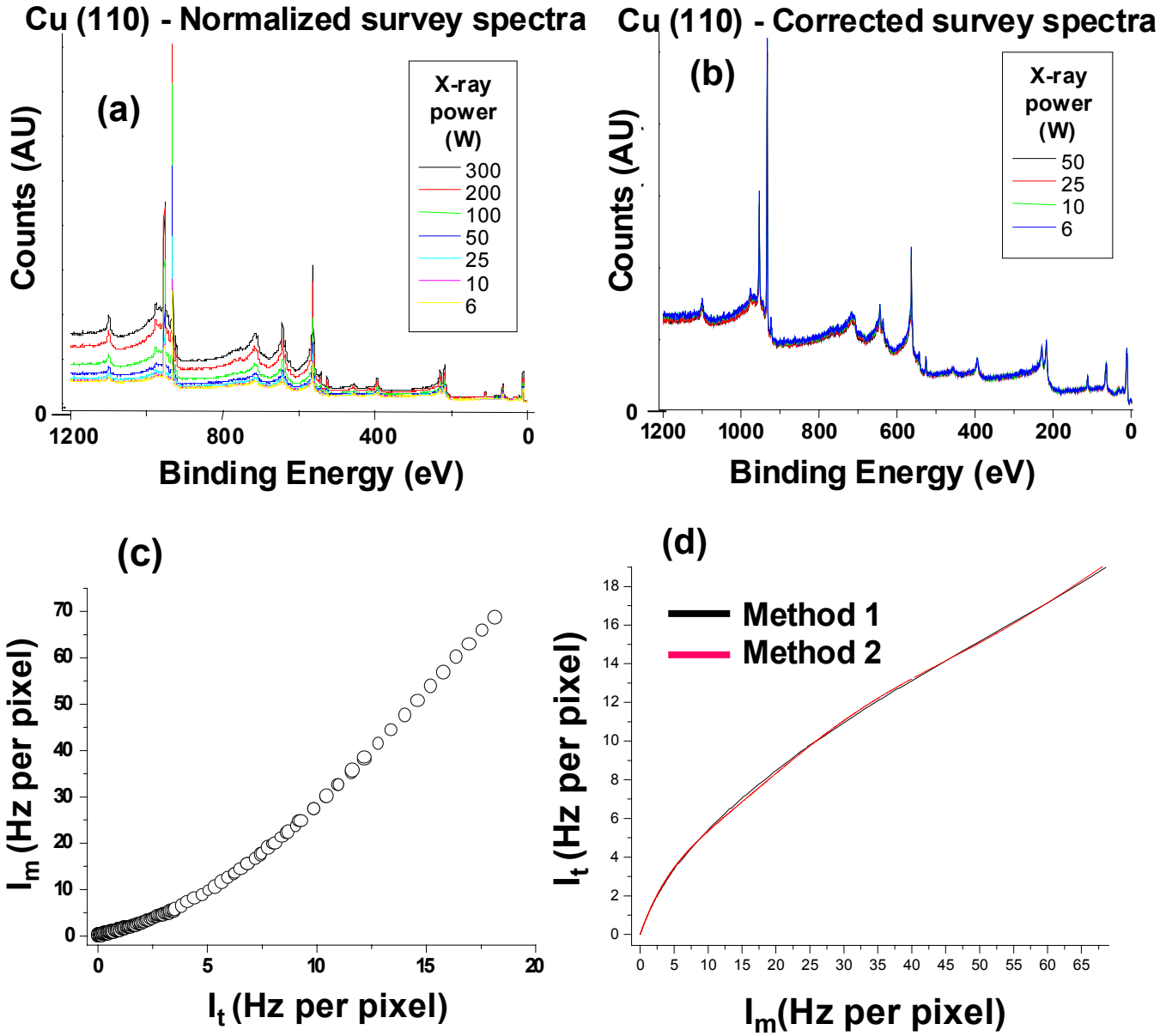

# Development and Evaluation of a New Liquid Cell System for Soft X-Ray Absorption Experiments

S. Matsuo[1], T. Kurisaki[2], H. Yamashige[2], P. Nachimuthu[3], R. C. C. Perera[4], and H. Wakita[1,2]
[1]Advanced Materials Institute, Fukuoka University, Nanakuma, Jonan-ku, Fukuoka 814-0180, Japan
[2]Department of Chemistry, Faculty of Science, Fukuoka University,
Nanakuma, Jonan-ku, Fukuoka 814-0180, Japan
[3]Department of Chemistry, University of Nevada Las Vegas, Las Vegas, NV 89154-4003, USA
[4]Center for X-ray Optics, Lawrence Berkeley National Laboratory, Berkeley, CA 94720, USA

## INTRODUCTION

Soft X-ray is well used as a means available to investigate the electron state of valence band in a material, because the energy of soft X-ray is close to that of the valence band and strongly affects the material in the electronic state. The soft X-ray absorption spectrum provides information on the electron states between the absorbing atom and neighboring atom(s) in a material, in addition, the researches by the soft X-ray absorption spectroscopy are extensively developed with the increase of the number of the target atoms for the researches, because the elements absorbing the soft X-ray include not only the light elements, but also the elements which can cause the L- and M-shells excitation. So far, for solid samples, the soft X-ray absorption spectroscopy has been utilized for the studies of developments for functional materials, the speciation of pollution compounds, the mechanistic analysis of catalytic reactions and vital functions [1]. However, for the soft X-ray absorption experiments for liquid samples, it has really been difficult to design the liquid cell system which is able to measure the absorption spectra under atmospheric pressure. In this paper, we report on a new liquid cell system for the soft X-ray absorption experiments developed at ALS, and show the X-ray absorption near-edge structure (XANES) spectra for aqueous Al salt solutions by the use of the cell system.

## APPARATUS

The setup of the developed cell system is depicted in Figure 1. This cell system has been installed in BL6.3.1, and has the vacuum system with two shutters to keep the pressure in the path, ca. $10^{-7}$ Torr. The window attached the silicon nitride ($Si_3N_4$) membrane, which has 150 nm in thickness and 1 mm square, is fixed on the end of the pressure path. A liquid sample is trapped between two other $Si_3N_4$ membrane windows, on which the polystyrene microspheres (ca. 10 μm in diameter) are dropped in advance. The liquid sample trapped is fixed on the sample holder, which is made of stainless steel and designed as the beam is transmitted by the sample liquid and detected by the silicon photodiode under the optimal condition, and then it is put on the sample stage. The end of the pressure path, sample stage, and detector are covered with the acryl case.

## EXPERIMENTAL

Aluminum K-edge XANES spectra were collected by a transmission mode using the cell system for aqueous solution samples and by a total electron yield method for powder samples pressed onto the conductive carbon tape. The measured aluminum compounds were aluminum chloride ($AlCl_3$), aluminum nitrate nonahydrate ($Al(NO_3)_3 \cdot 9H_2O$), sodium aluminate, and aluminum ethylenediaminetetraacetate (Al-EDTA) complex. The aqueous solution of Al-EDTA was

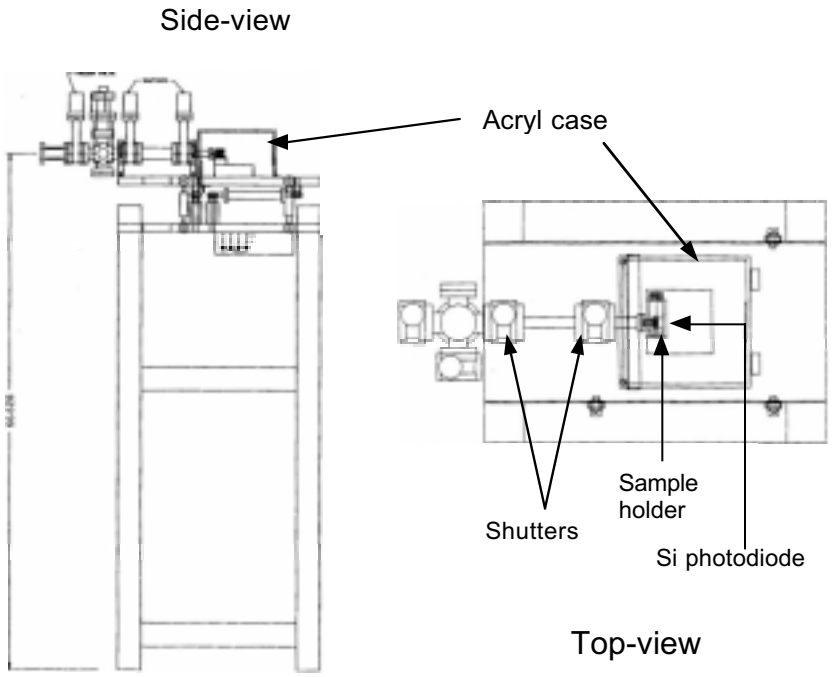


Figure 1. Setup of the XAFS cell system of soft X-ray absorption spectral measurements for solution samples.

prepared by adding 0.5 M $Al(NO_3)_3 \cdot 9H_2O$ aqueous solution (25 ml) to 0.5 M EDTA tripotassium salt aqueous solution (25 ml) and finally adjusted to pH 4.5. The other solution samples were high-concentrated aqueous solutions. Al-EDTA sodium salt dihydrate was purchased from DOJINDO Laboratories. Data were collected from 1550 to 1620 eV at intervals of 0.2 eV with the speed of 0.5 s a point. In the measurements, Helium gas was made to flow and to fill in the acryl case, which was covered with a black cloth.

## RESULTS

The Al K-edge XANES spectra for the aqueous solutions of $AlCl_3$, $Al(NO_3)_3 \cdot 9H_2O$, sodium aluminate, and Al-EDTA are shown in Figure 2 with those for their powder samples. In the powder samples, all the peak tops of the XANES spectra appear in almost similar energy position. In the aqueous solution samples, on the other hand, the peak tops of the XANES spectra of $AlCl_3$ and $Al(NO_3)_3 \cdot 9H_2O$ are similar in the position to those in their powder samples, while those of sodium aluminate and Al-EDTA are different from those in their powder samples, and shift to the low energy side. These results indicate that the coordination numbers for $AlCl_3$ and $Al(NO_3)_3 \cdot 9H_2O$ little change between the powder and aqueous solution samples, and those for sodium aluminate and Al-EDTA show a change. In fact, by the NMR study the coordination number of Al-EDTA has

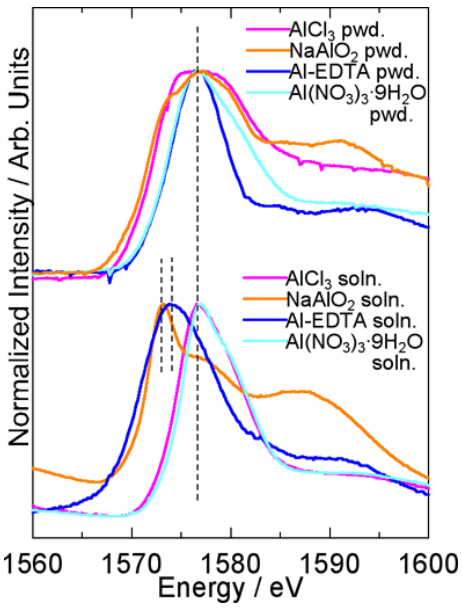


Figure 2. Al K-edge XANES spectra of powders and aqueous solution of various Al compounds.

been proposed to be six in powder and five in aqueous solution [2]. Accordingly, the peak position of the XANES spectra for Al-EDTA can be related with the coordination number. Furthermore, the relation between the peak position and coordination number would be also applied for all aluminum compounds.

## CONCLUSION

The new liquid cell system for the soft X-ray absorption experiments developed at ALS enables us to record the spectra characteristic of chemical species in solution. For the XANES spectra of aqueous aluminum salt solutions obtained by the liquid cell system, the change of the peak position was related with the coordination structure, especially coordination number.

## REFERENCES


1. H. Wakita, Bunseki (in Japanese) **1**, 24 (2002).
2. T. Yokoyama, Y. Tsuji, T. Kurisaki, and H. Wakita, presented at the IUPAC International Congress on Analytical Sciences 2001, Waseda University, Tokyo, Japan, 2001 (unpublished).



This work was supported by the Advanced Materials Institute, Fukuoka University and by the Director, Office of Energy Research, Office of Basic Energy Sciences, Materials Science Division, of the U.S. Department of Energy under Contract No. DE-AC03-76SF00098.



Principal investigator: Hisanobu Wakita, Advanced Materials Institute and Department of Chemistry, Faculty of Science, Fukuoka University. Email: wakita@fukuoka-u.ac.jp. Telephone: +81-92-801-8883.

# Distributed Experiment Control System (DECS) based on COM/DCOM technology.

G. Lebedev
Lawrence Berkeley National Laboratory, ALS, MS 7-222, Berkeley, CA 94720

In order to improve required time for automation of scientific experiments was developed integrated modular system based on COM/DCOM technology. For each software module assign associated task. All modules interaction and synchronization based on placing data and command in proprietary Real Time Data Server (RTDS).

System divides in four main layers:

1. Graphical User Interface (GUI) modules.
2. Device Drivers (DD) - support communication and executing command to external systems devices.
3. Element Controllers (EC) – provide primary command evaluation, data analysis and synchronization between DD.
4. Utility – support batch processing, login, error handling, file and database experiment recording, modules and devices monitoring, communication support with external distributed controlling systems (DECS or EPICS).

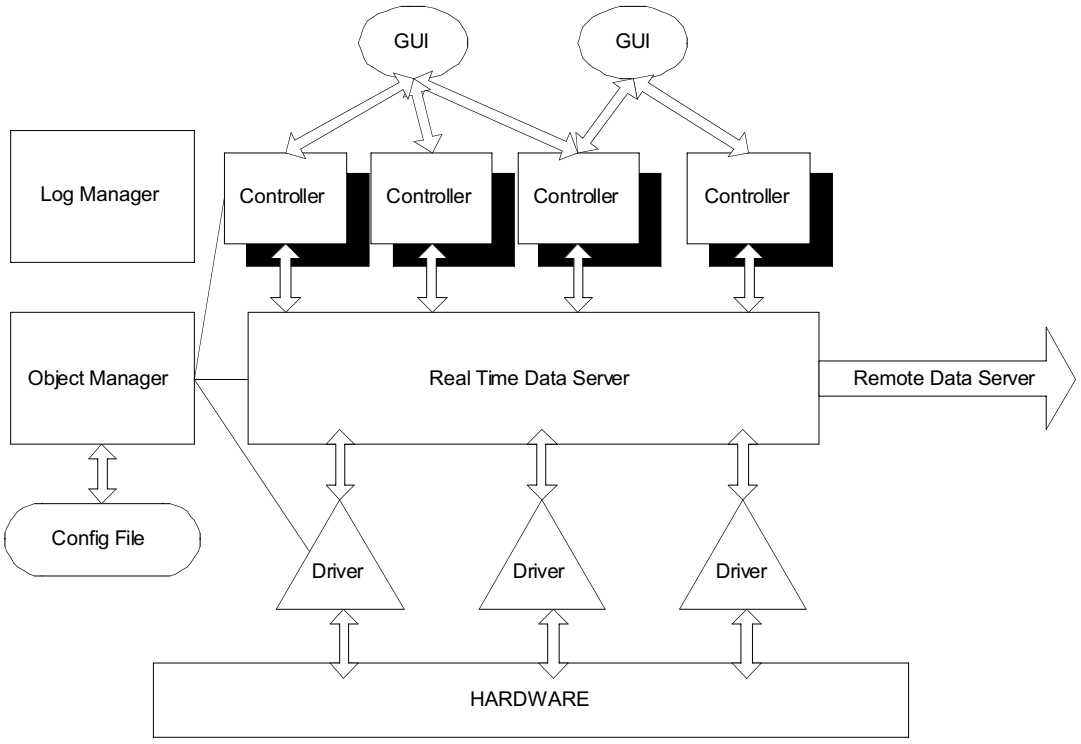

Configuration of the system accordingly to research station specification described in XML file, there every module presented as set of initialization parameters and structured records (data tags).

This modular structure allows for greater flexibility and extensibility as modules can be added and configured as required. Since each module is COM/DCOM-based, the control system is truly distributable in a highly object-oriented fashion. All modules can be resident on a single computer or spread across multiple computers networked together.

This work was supported by the Director, Office of Science, Office of Basic Energy Sciences, of the U.S. Department of Energy under Contract No. DE-AC03-76SF00098.

Principal investigator: Gennadi Lebedev, Lawrence Berkeley National Laboratory. Telephone: 510-486-4262. Email: gvlebedev@lbl.gov.

# New IR microscope and bench installed at BL1.4

Michael C. Martin[a], Hoi-Ying N. Holman[b], and Wayne R. McKinney[a]
[a] Advanced Light Source Division, Lawrence Berkeley National Laboratory, Berkeley, CA 94720
[b] Center for Environmental Biotechnology, Lawrence Berkeley National Laboratory, Berkeley, CA 94720

## 1. INTRODUCTION

New infrared spectromicroscopy equipment was purchased for and installed on the ALS infrared beamlines on beam port 1.4. It includes the latest step-scan capable FTIR bench and an infinity corrected infrared microscope which will allow for a number of new sample visualization methods. This equipment was purchased with funding from the DOE Office of Biological and Environmental Research (OBER) with the express purpose to develop biomedical and biological applications of synchrotron-based infrared spectromicroscopy.

## 2. EQUIPMENT

The new spectromicroscopy equipment includes a Thermo Nicolet Nexus 870 step- and rapid-scan FTIR bench, and a Thermo Spectra-Tech Continuum IR microscope, photographed below. The IR microscope includes two IR detectors, a wide-band MCT and a fast (20 ns) TRS MCT for time-resolved experiments. A fast digitizer (up to 100MHz) compliments the TRS MCT detector. The synchrotron beam coupled into the IR microscope continues to have a diffraction-limited spot size, thereby attaining a 200-fold increase in signal from small (3 – 10 micron) sample spot compared to a conventional thermal IR source. The infinity-corrected microscope optics allow for a number of additional sample visualization accessories which can help the user identify the important location within their sample for micro-IR analysis:

- Visual and IR polarizers
- Dark-field illumination
- DIC (Differential Interference Contrast) optics
- UV Fluorescence

An example of DIC optics enhancing a micrograph of human cheek cells is shown in the photograph to the right. The DIC technique provides a psuedo-3D effect, enhancing the contrast between different thicknesses of an otherwise clear sample. In the image to the right, one can make out the nuclei of the cells (thicker bump near the middle of each cell), whereas this would be difficult using conventional illumination.

This new instrument will aide in user scientific research across many fields. For example, the study of individual living cells, toxic contaminants, bioremediation, protein microcrystals, rhizoids, and forensic evidence will all be enhanced by the additional capabilities of this new SR-FTIR spectromicroscopy system.

**ACKNOWLEDGEMENTS**

This research was supported by the Office of Science, Office of Biological and Environmental Research, Medical Science Division and the Office of Science, Office of Basic Energy Sciences, Materials Sciences Division, of the U.S. Department of Energy under Contract No. DE-AC03-76SF00098 at Lawrence Berkeley National Laboratory.

Principal investigator: Michael C. Martin, Advanced Light Source Division, LBNL, 510-495-2231, MCMartin@lbl.gov

# Response of an Active Pixel Sensor (APS) Detector to 1.5 GeV Electrons

H.S. Matis,[1] H. Bichsel,[2] F. Bieser,[1] S. Kleinfelder,[1] and H.H. Wieman[1]
[1]Nuclear Science Division, Ernest Orlando Lawrence Berkeley National Laboratory,
University of California, Berkeley, California 94720, USA
[2]Physics Department,
University of Washington, Seattle, Washington 98185, USA

## INTRODUCTION

There is tremendous interest in ultra-relativistic heavy ion physics to measure open charm – particles with the charmed quark. Charmed particles provide a more direct link with the early hot Quark Gluon phase of the Nucleus-Nucleus interaction. Most of the particles currently available for measurement in these experiments primarily reflect the later hadronization phase of the interaction. Due to their larger mass, charmed quarks only can be produced during the hot partonic phase, so they provide a more direct connection to this early stage without contamination from the later cooler phase. With the help of a new inner high-resolution vertex detector, we can measure the charm content through the D meson decay channel.

Accomplishing this requires a vertex detector with very good pointing resolution. This means the vertex detector must be very thin to reduce multiple scattering. It also means the vertex detector must have excellent two hit resolution so that it can be placed very close to the interaction without being compromised by the huge particle numbers, i.e. it must have a high pixel density.

## PREVIOUS WORK

Experiments that are under construction at the Large Hadron Collider at CERN use Silicon Pixel diode wafers bump bonded to the readout electronic chips. [1] This approach does not meet the thinness and high pixel density requirements for the STAR experiment [2] at Brookhaven National Laboratory. An alternative technology that addresses these issues is the integration of special amplifier and logic structures required for readout directly into the high resistive silicon of the detector. Researchers have made some progress in this approach, but it will always be limited by the need for special processes. This approach increases the cost and mandates the complication of dealing with specialized foundries.

Work [3] at LEPSI in Strasbourg has demonstrated that Active Pixel Sensor (APS) technology in CMOS works very well for detecting minimum ionizing particles with a good signal to noise ratio. However, APS technology is in its infancy, so that we must study many issues to create a working high-resolution pixel detector.

## TEST SETUP

We designed a prototype sensor array that includes an array of 128 by 128 pixels broken into four quadrants of 64 by 64 pixels. Each quadrant uses a different sensor structure and/or readout circuit. Each pixel is 20 by 20 microns in size, and the entire array is about 2.5 mm on a side. Quadrant 1 has a single diode to pick up the charge from the chip while quadrant 2 had four

diodes. Due to the larger capacitance of quadrant 4, the signal size is less than quadrant 1. In this article, we will report on the results from quadrant 1.

We mounted the APS chip on a readout board and used a 2 MHz pipelined ADC, which digitized the data. A Xilinx XC3064A FPGA provided the control signals for reading out the APS chip and sent the data to a National Instruments PCI-DIO-32HS PCI interface located in a Macintosh G3 computer. A 16 K x 16 FIFO chip between the ADC and the DAQ interface provided an elasticity buffer to guarantee consistent readout timing.

While the ALS was in the storage ring mode, the booster was used to deliver 1.5 GeV electrons to our detector at a rate of 1 Hz. We put our detector at the end of branch line off the main booster-to storage ring (BTS) transfer line. There was about 20 cm of air between our detector and the last vacuum gate valve. We set the intensity of the beam so that each beam pulse provided on the order of 10 particles to our detector. The left graph of Fig. 1 shows the response of Quadrant 1 of the detector to one beam spill. This graph shows several easily identified electrons. The figure on the right shows the same detector when the beam was off.

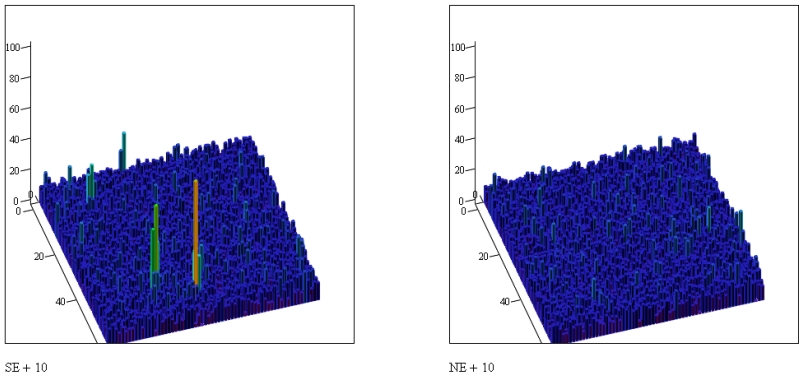


Figure 1. The graph on the left shows the response of the detector to 1.5 GeV electrons, while the graph on the right shows the results when the beam was turned off. Each rectangle represents on pixel on the chip. The height of each rectangle represents the energy deposited in each pixel.

## RESULTS

To eliminate the noise introduced by resetting the chip, we used the correlated double sampling method to analyze the data. We reset the chip and then read out the value of the pixels one frame before the beam hit the detector, we then read the chip again and subtracted the two frames. The result is the charge deposited by electron beam plus the leakage current. We then subtracted a subsequent frame to eliminate the leakage current.

Figure 2 shows the energy normalized ADC spectrum for this run. The solid curve shows an absolute calculated energy assuming that all charge comes from the 8 μm epitaxial layer of the chip. The nose, which is 17 electrons, is subtracted from this spectrum. The fit is in excellent agreement with the expected result. The peak of the energy distribution is near 500 electrons. We are currently producing the next version of the chip and plan on testing it in the same ALS beam line.

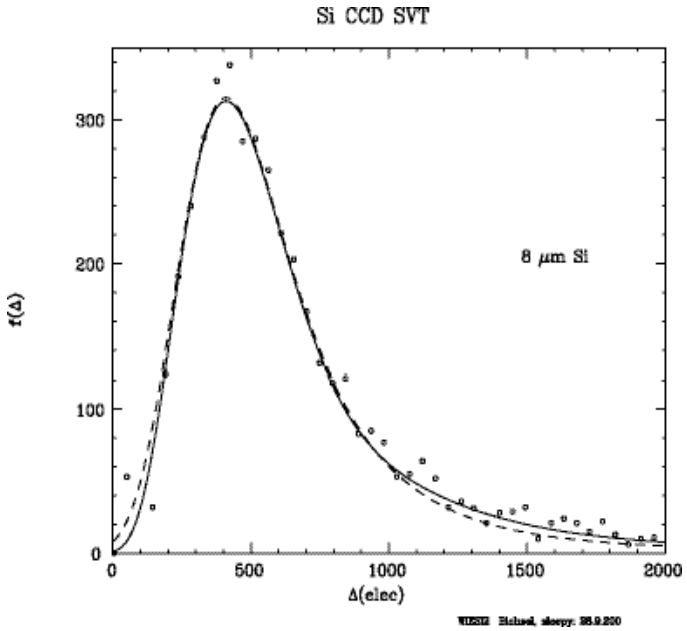


Figure 2. Prototype device test results fitted to a 1.5 GeV electron spectrum.

## ACKNOWLEDGMENTS

We would like to thank Ali Belkacem and Gary Krebs who guided us through the planning process and taught us how to use the ALS beam line. Because of their generous effort, we quickly setup up our apparatus and finished our tests. We also wish to thank the rest of the ALS Staff who provided us with the logistics necessary to make these measurements.

## REFERENCES

1. ALICE Technical Design Report of the Inner Tracking System (ITS), CERN/LHCC 99-12, ALICE TDR 4 (1999).
2. See http://www.star.bnl.gov
3 R. Turchetta *et al.*, Nucl. Instrum. and Methods A **458**, 8 (2001).

The Director, Office of Energy Research, Office of High Energy and Nuclear Physics, Nuclear Physics Division, of the U.S. Department of Energy under Contract No, DE-AC03-76SF00098 supported this work.

Principal investigators: Howard Matis and Howard Wieman, Nuclear Science Division, Ernest Orlando Lawrence Berkeley National Laboratory. Email: hsmatis@lbl.gov and hhwieman@lbl.gov Telephone: 510-486-5031 and 510-485-2473.

# Transmission Functions of a Scienta SES-200 Hemispherical Analyzer.

S.E. Canton[1,2], J.D. Bozek[1], N. Berrah[2]

[1] Lawrence Berkeley National Laboratory, Advanced Light Source,
University of California, Berkeley CA 94720.
[2] Department of Physics, Western Michigan University, Kalamazoo MI 49008.

## INTRODUCTION

Most of the information extracted from photoelectron spectra comes from the relative comparison of line intensities. As the range of kinetic energy in experiments carried out at synchrotron light sources is usually wide, the transmission function of the electron energy analyzer must be accounted for. The transmission functions of a Scienta SES-200 hemispherical analyzer have been determined for different pass energies (5,10,20 and 40 eV). The method is based on the measurement of the intensity ratio between photoelectron lines with dispersing kinetic energy and the corresponding Auger lines with constant kinetic energy. The standard Auger line intensities of the Xe $N_{4,5}OO$ spectrum have been obtained and used as a test of the reliability of the correction procedure.

## RESULTS

The method proposed in [1] is based on the measurement of the intensity ratio between photoelectron lines and Auger lines related to the decay of the same core-hole vacancy using tunable synchrotron radiation. Because of their constant kinetic energy, the Auger lines have a constant transmission, whereas the photoline intensity reflects the relative transmission of the spectrometer.

In the present work, the transmission function F is given by the ratio of the $4d_{5/2}$ photoline in Xenon and some selected Auger lines $N_5OO$.

$$F_{5/2}(E_{kin}) = I_{4d_{5/2}}/(I_{51}+I_{52}+I_{53})$$

In order to include the ratio of the $4d_{3/2}$ photoline and the corresponding Auger lines $N_4OO$, a scaling factor R needs to be calculated using the ratio taken at high photon energy.

$$F_{3/2}(E_{kin}) = R*I_{4d_{3/2}}/(I_{41}+I_{42}+I_{43})$$

The resulting transmission curves are shown in Fig.1.

The lines were fitted with a modified Voigt profile accounting for Post Collision Interaction (PCI) distortion. All the Auger lines belonging to the same group were constrained to have equal width and asymmetry. The relative intensities once corrected agree well with the values in the literature [2].

## REFERENCES

[1] J. Jauhianen J Elect Spectrosc Relat Phenom. **69** (1994) 181-187
[2] L.O. Werme et al, Phys. Scr. **6** (1972) 141

This work was funded by the Department of Energy, Office of Science, Basic Energy Sciences, Chemical and Material Science Division, under the contract No. DE-AC03-76SF00098.

Principal investigator: Nora Berrah, Physics Dept., Western Michigan University, 616-387-4955, berrah@wmich.edu.

Fig.1 Transmission functions for 5, 10, 20 and 40 eV pass energy.